Chemical Engineering Journal 158 (2010) 207–212

Contents lists available at ScienceDirect

Chemical Engineering Journal

journal homepage: www.elsevier.com/locate/cej

In situ characterization of local hydrodynamic parameters in closed-loop aeration tanks

Yannick Fayolle[a,*], Sylvie Gillot[a], Arnaud Cockx[b], Laetitia Bensimhon[a], Michel Roustan[b], Alain Heduit[a]

[a] *Cemagref, UR HBAN, Parc de Tourvoie, BP 44, 92163 Antony Cedex, France*
[b] *INSA – LISBP, 135 Avenue de Rangueil, 31077 Toulouse Cedex 4, France*

ARTICLE INFO

Article history:
Received 24 April 2008
Received in revised form
22 December 2009
Accepted 30 December 2009

Keywords:
Aeration
Bubble size
Gas hold-up
Horizontal flow systems
Wastewater treatment

ABSTRACT

The objective of this experimental study was to collect and to interpret data in order to better understand the oxygen mass transfer phenomena occurring in full-scale aeration tanks equipped with fine bubble diffusers and slow speed mixers (inducing horizontal liquid flows). Bubble size, local depth and oxygen mass transfer coefficient were measured *in situ* for a given air flow rate ($1555\,N\,m^3\,h^{-1}$) and for two different axial liquid velocities. The increase in the global oxygen transfer coefficient is of 29% when the mean axial liquid velocity varies from 0 to $0.42\,m\,s^{-1}$. The small influence of the liquid velocity on the local bubble Sauter diameter (about −4%) cannot explain the increase in k_La_{20}. This increase in k_La_{20} with the axial liquid velocity is mainly due to the attenuation of the vertical liquid circulation induced by the gas injection.

1. Introduction

Activated sludge systems are widely used in wastewater treatment. In such processes, aeration can represent up to 70% of the energy expenditure of the all plant. In order to minimise this consumption and to improve the treatment efficiency, optimising aeration devices is essential.

To this aim, syntheses of measurements performed on full-scale aeration tanks pointed out the main parameters affecting oxygen transfer in clean water [1,2]. In addition, computational fluid dynamics (CFD) is more and more used to interpret the obtained results [3–6]. However, no set of data including all the parameters required to understand and to simulate the phenomena (bubble size as input data; gas hold-up, axial liquid velocity and oxygen transfer coefficients as validation data) has ever been proposed for full-scale closed-loop aeration tanks.

In situ measurements (bubble size, axial liquid velocity, oxygen transfer coefficient, local depth) have therefore been performed on full-scale plants, in order to obtain precise information on the physical phenomena occurring in closed-loop aeration tanks and to optimise their operation. The objective of this paper is to present and to analyse the obtained results.

2. Materials and methods

Measurements have been performed on a full-scale aeration tank. The development of the measurement methods is described in detail in a previous paper [7].

2.1. Aeration tank

The studied basin was chosen as representative of close-loop reactors with classical configuration and water depth. The aeration tank is of annular type (volume of liquid $[V] = 1493\,m^3$; internal diameter $[D_{in}] = 7.83\,m$; external diameter $[D_{out}] = 20.25\,m$; water depth $[d_w] = 5.45\,m$), and is equipped with six grids of 26 fine bubble EDPM membrane diffusers (tubes of 0.8 m length) and one large blades slow speed mixer (2.5 m diameter), mounted at the bottom of the tank (Fig. 1). The tank was filled with tap water.

Each grid of diffusers is divided into two zones of equal surface with a different diffuser density (10 tubes in the zone near to the inner diameter of the tank and 16 tubes in the zone near to the outer diameter).

In the following, the grids of diffusers are designed by a number corresponding to their location. As example, grid 2 corresponds to the second grid in the direction of the liquid flow, indicated by the arrow in Fig. 1.

* Corresponding author. Tel.: +33 1 40 96 60 32; fax: +33 1 40 96 61 99.
E-mail address: yannick.fayolle@cemagref.fr (Y. Fayolle).

1385-8947/$ – see front matter © 2010 Elsevier B.V. All rights reserved.
doi:10.1016/j.cej.2009.12.043

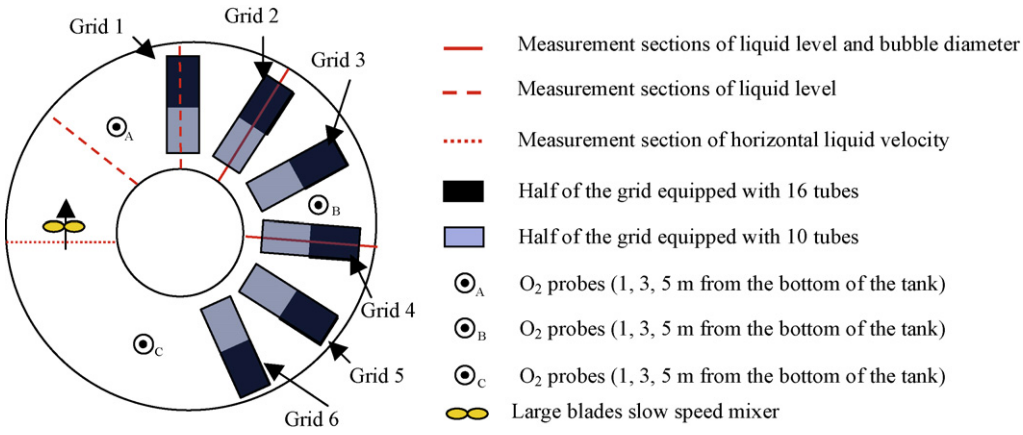

Fig. 1. Annular loop reactor.

2.2. Axial liquid velocity measurement

The axial liquid velocities were determined with and without aeration using an electromagnetic flow-meter (corresponding to one point/m^2 of section, [8]) on 35 points regularly distributed on one vertical section of the tank away from the bubble plume (Fig. 1). The measurement section was orthogonal to the flow direction.

The mean velocity represents the arithmetic average of the local velocities obtained on the 35 measurements points. The sampling time was fixed to 60 s, and allows determining the local liquid velocity with a confidence interval of ±3%.

2.3. Oxygen transfer coefficient measurement

The oxygen transfer coefficient was determined according to the non-steady state method integrated in the American and European standards [9,10]. The method consists of monitoring the dissolved oxygen concentration increase after the addition of sodium sulfite in the presence of a catalyst (cobalt chloride).

For each measurement, the addition of sodium sulfite was performed without aeration. Appropriate mixing was provided by built-in mixers to prevent settling of the sulfite powder and to allow a uniform distribution of the reactant.

The dissolved oxygen concentration was measured on 9 points using dissolved oxygen probes (YSI 57), located on 3 water depths (1, 3 and 5 m from the bottom of the tank), on 3 verticals (see Fig. 1). The sampling frequency was set to 5 s. The oxygen transfer coefficient was then deduced from the obtained curves using a non-linear regression analysis.

In the following, the oxygen transfer coefficient is expressed at standard conditions (20 °C, 1013 hPa) as follows:

$$k_L a_{20} = k_L a_T \times 1.024^{20-T} \quad (1)$$

where $k_L a_T$ is the oxygen transfer coefficient at the temperature T (°C), $k_L a_{20}$ is the oxygen transfer coefficient at 20 °C.

2.4. Bubble size measurement

Bubble diameters were determined from images obtained by an immersed camera (Canon Powershot G6) inserted in a waterproof Plexiglas box located in the bubble plume (see Fig. 2). Lighting was carried out by two 600 W spots mounted on the immersed structure, on both sides of the camera. The scale for the bubble size determination was obtained with the help of a ruler placed in front of the lens. Only the sharp bubbles located in the plan of the ruler are taken into account in the bubble size determination.

Fig. 2. Bubble size measurement tool.

The bubbles (Fig. 3) have an ellipsoid shape in clean water, and an equivalent diameter, $d_{eq,i}$, is defined as the diameter of a spherical bubble having the same volume as the ellipsoid, as follows:

$$d_{eq,i} = \sqrt[3]{a_i^2 . b_i} \quad (2)$$

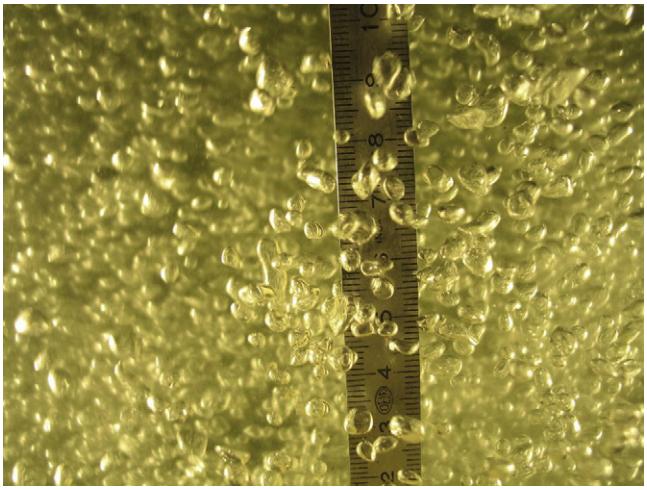

Fig. 3. Typical picture obtained in the bubble plume.

Table 1
Experimental conditions [Q_T = total air flow rate, Q_{surf} = surface air flow rate (air flow rate divided by the area covered by the diffuser grids, see Ref. [2]) and S_P = surface area of the perforated membranes].

Case	Q_T (N m^3 h^{-1})	Q_{surf} (N m^3 h^{-1} m^{-2})	Q_T/S_P (N m^3 h^{-1} m^{-2})	Mixing
1	1555	29	85	No
2	1555	29	85	Yes

where a_i and b_i are respectively the major and the minor axis of the ellipsoidal bubble i (m).

An image analysis software package (ImageJ, http://rsb.info.nih.gov/ij/) was used to obtain the equivalent diameter of each bubble.

The Sauter diameter (d_S), required to determine the gas–liquid interfacial area, was calculated as follows:

$$d_S = \frac{\sum_{i=1}^{N} d_{eq,i}^3}{\sum_{i=1}^{N} d_{eq,i}^2} \quad (3)$$

where $d_{eq,i}$ is the equivalent diameter of bubble i and N is the total number of bubbles.

The determination of the Sauter diameter requires size determination of a minimum of 100 bubbles [7].

Pictures were taken on two sections above two different grids (Fig. 1) with and without mixing (note that the measurement sections were not changed with the horizontal velocity to follow the bubble plume). On each measurement sections, bubble sizes were determined on 9 points (3 vertical distances from the diffusers and 3 distances from the internal wall).

2.5. Local depth measurement

On four vertical sections of the tank (orthogonal to the flow direction and located in and out of the bubble plume, as indicated in Fig. 1), the local depth was measured using a magnetostrictive level meter KTEK AT100, on 5 points on each section (1–5 m from the external wall). The measuring apparatus consists in a float, which follows the movements of the free surface and slides along a sensing tube.

The sampling time was fixed to 380 s. This sampling time allows estimating the average local depth with a confidence interval of ±5%.

3. Results and discussion

Measurements were performed at one total air flow rate, without and with mixing. Table 1 presents the experimental conditions.

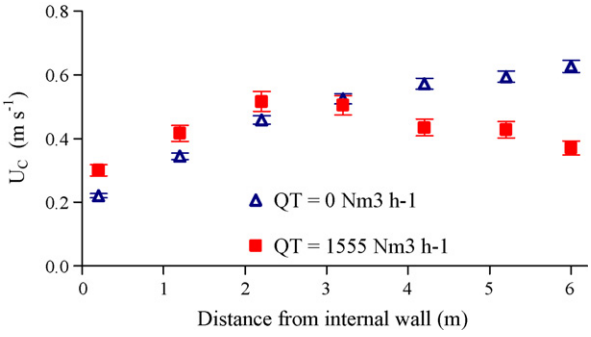

Fig. 4. Mean horizontal velocities (integrated on the measurement verticals) versus distance from internal wall, without (Δ) and with aeration (■).

Table 2
Mean circulation velocities ($U_{C\,mean}$) in one measurement section, without and with aeration (the variation represents the variation of the mean axial liquid velocity between Q_T = 0 N m^3 h^{-1} and Q_T = 1555 N m^3 h^{-1}).

Q_T (N m^3 h^{-1})	$U_{C\,mean}$ (m s^{-1})	Variation (%)
0	0.48	–
1555	0.42	−13

3.1. Axial liquid velocities

Axial liquid velocities were measured in one section without and with aeration. Fig. 4 presents the local axial liquid velocities (U_C) as a function of the distance from the internal wall (on the measurement section). Each point corresponds to the average of the 5 local velocities measured on 1 vertical.

Without aeration, the axial liquid velocity increases from 0.22 to 0.63 m s^{-1} from the internal wall to the external one. With aeration, U_C increases up to the distance of 2.2 m from the internal wall (from 0.30 to 0.52 m s^{-1}), and decreases to 0.37 m s^{-1} on the other part of the section.

Aeration induces head losses and therefore disturbs the liquid flow. As the grids of diffusers are divided into two sections of different diffuser density (Fig. 1), the deformation of the velocity field is more important near to the external wall than to the internal one.

Table 2 presents the arithmetic average of the local velocities obtained on the 35 measurement points.

Without aeration, the mean liquid circulation velocity is of 0.48 m s^{-1}. This value is more important than the minimal velocity recommended by Déronzier and Duchêne [8] in order to optimise aeration performances and to ensure the absence of settling (0.35 m s^{-1}).

The gas injection involves a decrease in the mean liquid circulation velocity of 13%.

3.2. Influence of the axial liquid velocity on the global oxygen transfer coefficient (k_La_{20})

Dissolved oxygen (DO) concentration evolutions versus time are presented without and with mixing, respectively in Figs. 5 and 6.

Whatever the experimental conditions, the DO concentration is the same at different heights of the tank (1 and 5 m from the bottom of the basin in the example of Figs. 5 and 6). Therefore the aeration tank could be considered as a perfectly mixed reactor for the liquid phase. The oxygen transfer coefficient deduced from these

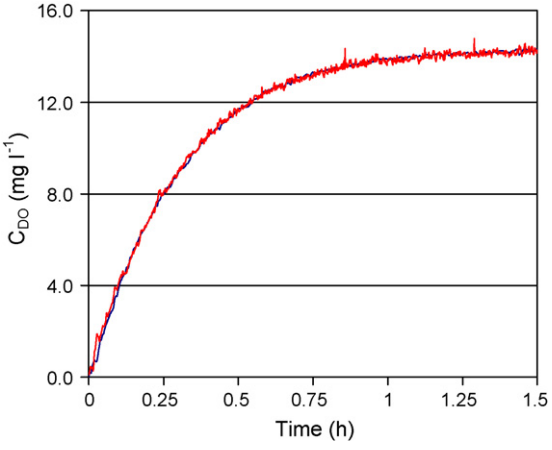

Fig. 5. Dissolved oxygen concentration (C_{DO}) versus time during reoxygenation (1 m [■] and 5 m [■] from the bottom of the tank) without mixing (case 1). (For interpretation of the references to color in this figure legend, the reader is referred to the web version of the article.)

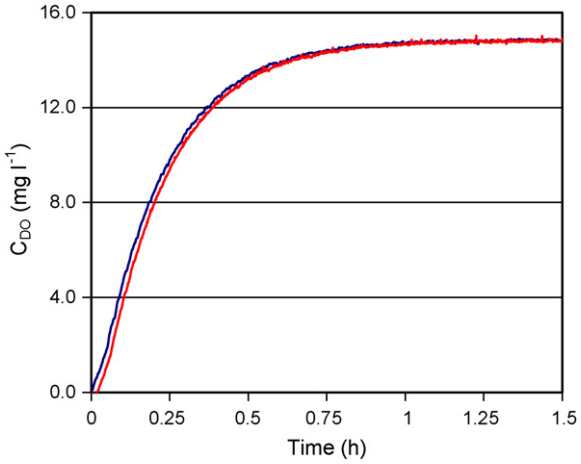

Fig. 6. Dissolved oxygen concentration (C_{DO}) versus time during reoxygenation (1 m [■] and 5 m [■] from the bottom of the tank) with mixing (case 2). (For interpretation of the references to color in this figure legend, the reader is referred to the web version of the article.)

Table 3
Axial liquid velocity and oxygen transfer coefficient (the variation represents the variation of the standard oxygen transfer coefficient between $U_{C\,mean} = 0\,m\,s^{-1}$ and $U_{C\,mean} = 0.42\,m\,s^{-1}$).

Case	$U_{C\,mean}$ ($m\,s^{-1}$)	k_La_{20} (h^{-1})	Variation (%)
1	0	5.39	–
2	0.42	6.93	+29

curves is a global mass transfer coefficient that does not take into account potential local variations in the parameters governing oxygen transfer such as observed by Giovannettone and Gulliver [11] in a full-scale airlift reactor.

The deduced oxygen transfer coefficients obtained for the two sets of experimental conditions are presented in Table 3. Applying a mean axial liquid velocity of 0.42 m s^{-1} enhances the oxygen transfer by 29%. This enhancement is in the lower range of those obtained on other sites (from 30% to 50%, [12]).

3.3. Influence of the axial liquid velocity on the bubble size

3.3.1. Local diameter

On each measurement section (Fig. 1), bubble sizes were determined on 9 points (for 3 vertical distances from the diffusers and 3 distances from the internal wall).

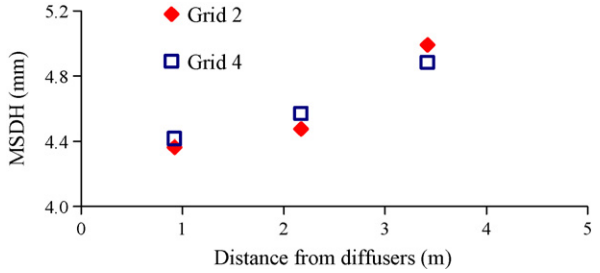

Fig. 7. Evolution of the MSDH with the vertical distance from the diffusers without mixing.

Equivalent local bubble diameters are presented in Tables 4 and 5 for the two studied grids, the 9 sampling points and the 2 operating conditions (without and with mixing).

For grid 2, without mixing, the local Sauter diameter ranges from 4.1 to 5.3 mm for a vertical distance to diffusers from 0.92 to 3.42 m. For a mean axial liquid velocity about 0.42 m s^{-1}, this value is comprised between 4.0 and 4.8 mm.

The evolution of the local Sauter diameter is equivalent for Grid 4.

For each grid and distance from the internal wall and whatever the operating conditions, the local Sauter diameter increases with the vertical distance from the grid of diffusers.

3.3.2. Mean Sauter diameter on a horizontal (MSDH)

The mean Sauter diameter on a horizontal (MSDH) is introduced in order to investigate the evolution of the bubble diameter as a function of the vertical distance from the grid of diffusers.

The evolutions of MSDH as a function of the vertical distance from the diffusers without and with mixing are presented in Figs. 7 and 8. For any distance from the diffusers, MSDH does not depend on the studied grid.

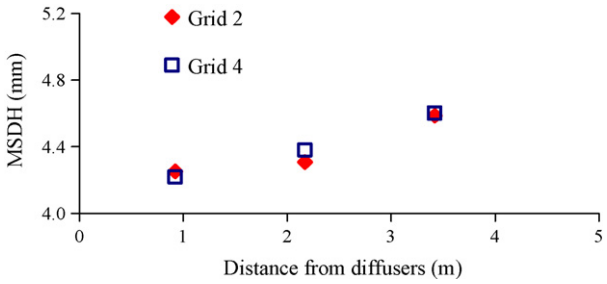

Fig. 8. Evolution of MSDH with the vertical distance from the diffusers with mixing.

Table 4
Local Sauter diameter (in mm) as a function of the mean axial liquid velocity and of the measurement point for grid 2.

UC mean ($m\,s^{-1}$)		0			0.42		
Horizontal distance from internal wall (m)		1	3	5	1	3	5
Vertical distance from diffusers (m)	3.42	4.8	4.7	5.3	4.8	4.3	4.6
	2.17	4.3	4.4	4.7	4.5	4.3	4.2
	0.92	4.1	4.4	4.6	4.5	4.0	4.3

Table 5
Local Sauter diameter (in mm) as a function of the mean axial liquid velocity and of the measurement point for grid 4.

$U_{C\,mean}$ ($m\,s^{-1}$)		0			0.42		
Horizontal distance from internal wall (m)		1	3	5	1	3	5
Vertical distance from diffusers (m)	3.42	5.2	4.6	4.8	4.6	4.6	4.6
	2.17	4.6	4.7	4.4	4.2	4.5	4.4
	0.92	4.4	4.4	4.4	4.1	4.3	4.3

Table 6
Global Sauter diameter versus mean axial liquid velocity for the two studied grids.

$U_{C\,mean}$ (m s^{-1})	GSD (mm)	
	Grid 2	Grid 4
0	4.6	4.6
0.42	4.5	4.4

During the rise of the bubbles from 0.92 and 3.42 m from the diffusers, MSDH increases from 4.4 to 5.0 mm without mixing, and from 4.2 to 4.6 mm with mixing.

This increase (+5.4%/m and +3.8%/m, respectively without and with mixing) is higher than the evolution due to the hydrostatic pressure decrease (+3.1%/m), especially without mixing.

3.3.3. Global Sauter diameter (GSD)

The Global Sauter diameter (GSD) is calculated from the equivalent diameters resulting from the 9 measurement points on one section. This parameter is introduced in order to characterise the mean bubble size and the influence of the mean axial liquid velocity on it.

GSD values are presented for each operating conditions and for the two measurements sections in Table 6.

The order of magnitude of the Global Sauter diameter is about 4.5 mm. This value is higher than the one usually measured on pilot scale (from 2.5 to 4.0 mm for EDPM membrane diffusers [13–15] and than the one used to simulate hydrodynamics and oxygen transfer in aeration tanks [4,16]. This order of magnitude of the average bubble size is the same as the one observed in bubble columns. Significantly lower values have been measured in a deep airlift reactor [17].

Moreover, the Global Sauter diameter slightly decreases with the axial liquid velocity (−4% between measurements without and with mixing).

3.4. Influence of the axial liquid velocity on the local depth

Local depths were measured on each point without and with aeration. The results are expressed using the following ratio (R_H):

$$R_H = \frac{H - H_0}{H} \quad (4)$$

where H_0 is the liquid depth without aeration and H is the mixture depth with aeration (m), both measured at one point.

Non-negligible variations of the local depth were measured out of the aerated zone, highlighting gradients of liquid dynamic pressure due to mechanical mixing and to a non-uniformly distributed air injection system. For example on a section located out of the aerated zone (see Fig. 9), the R_H factor is comprised between −0.18% and −0.01% without mixing and between −0.36% and 0.13% with mixing.

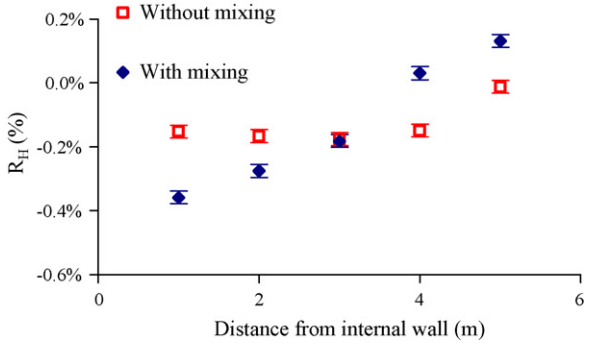

Fig. 9. R_H measured on the section out of the bubble plume, without (□) and with mixing (◆).

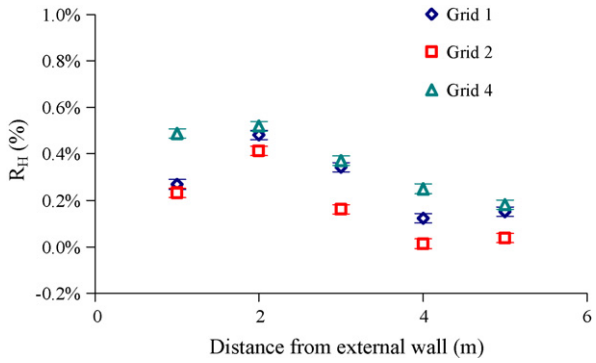

Fig. 10. R_H for sections corresponding to grids 1, 2 and 4, without mixing.

If the level increase due to aeration was uniform (such as in bubble columns), R_H would be an estimate of the gas hold-up. On full-scale aeration tanks, R_H is therefore only considered as a qualitative indicator of the bubble dispersion into the liquid.

R_H values obtained on the three sections located in the aerated zone (close to grids 1, 2 and 4, see Fig. 1), without and with mixing, are presented in Figs. 10 and 11.

Without mixing (Fig. 10), R_H values vary from 0.12% to 0.48% on grid 1, from 0.01% to 0.41% on grid 2 and from 0.18% to 0.52% on grid 4.

This profile is not regular, with R_H values more important near to the internal wall. This may be due to the different diffuser density (see Fig. 1). Considering a homogeneous distribution of the air flow rate per diffuser, the difference in the diffuser density on a grid induces a more important surface air flow rate near the internal wall. The difference of density of water column, induced by the surface air flow rate gradient, creates important spiral flows that move the bubble plume towards the internal wall.

With mixing (Fig. 11), R_H values increase with the distance from the internal wall from −0.04% to 0.19% on grid 1, from 0.25% to 0.84% on grid 2 and from 0.18% to 0.46% on grid 4. R_H values are higher near to the external wall. The horizontal flow seems to reduce the above mentioned spiral flows, creating a R_H profile more in agreement with the diffuser density.

3.5. Discussion

Applying a mean axial liquid velocity of 0.42 m s^{-1} on a real scale annular loop reactor (1500 m^3) enhances the oxygen transfer coefficient from 5.39 to 6.93 h^{-1} (+29%). Similar enhancements have been attributed to:

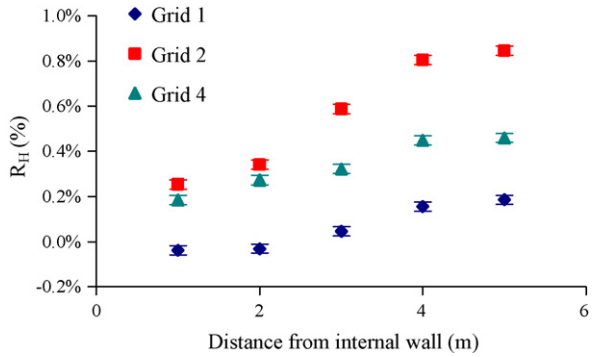

Fig. 11. R_H for sections corresponding to grids 1, 2 and 4, with mixing.

- The shearing effect due to the axial liquid velocity, inducing a reduction in the size of the nascent bubbles [18,19];
- the neutralisation of the vertical liquid circulation ("spiral flows") by the axial liquid flow. The spiral flows are produced at the edges of the aerated zones by the bubble rise (drag effect) and increase the bubble rising velocity. Neutralising them thus increases the gas/liquid contact time [4,20].

The measured decrease in the Global Sauter diameter when applying the horizontal velocity is of 4%. The relatively small influence of the liquid velocity on the Sauter diameter could not explain the increase in the global oxygen transfer coefficient when the axial liquid velocity varies from 0 to 0.42 m s^{-1}. The increase in the oxygen transfer coefficient with the mean axial liquid velocity is therefore mainly due to the partial neutralisation of the vertical liquid circulation induced by the gas injection, and thus to the linked gas hold-up increase.

Moreover, computational fluid dynamics (CFD) is more and more used to optimise aeration systems [3,4,6]. However, these studies are facing a lack of bubble size measurements on full-scale tanks which is the dominating parameter of the oxygen transfer phenomena. The use of an arbitrary bubble diameter as input data thus prevents from using the oxygen transfer coefficient as a validation criterion. The bubble size has a strong impact on the oxygen transfer coefficient by modifying:

- the gas/liquid interfacial area (a) which is inversely proportional to the bubble diameter;
- the liquid phase oxygen transfer coefficient (k_L): it depends on the thickness of the boundary layer around the bubble and the bubble size.

The work presented here will therefore be of high interest to simulate more accurate oxygen transfer using CFD tools.

4. Conclusions

A set of local data including all the required parameters to understand and to simulate fluid dynamics and oxygen transfer has been proposed for full-scale plants. Axial liquid velocities, oxygen transfer coefficients, bubble sizes and local depths have been determined *in situ* on a full-scale aeration tank. The main conclusions are as follows.

The order of magnitude of bubble Sauter diameter of 4.5 mm has been evaluated and seems to be not dependent on the studied grid.

Applying an axial liquid velocity causes an enhancement of the oxygen transfer coefficient (+29%). This enhancement is mainly due to gas hold-up increase, as the influence of the axial liquid velocity on the bubble Sauter diameter is slight (−4%).

Finally, this study contributes to a better comprehension of the particular hydrodynamics and oxygen transfer phenomena in aerated tanks and could be used in order to predict aeration capacity using computational fluid mechanics.

Acknowledgements

The authors are grateful to the persons that have been involved in the experimental measurements on full-scale aeration tanks.

References

[1] J.A. Mueller, W.C. Boyle, H.J. Pöpel, Aeration: Principle and Practice, Water Quality Management Library, 2002, 353 pp.
[2] S. Gillot, S. Capela-Marsal, G. Carrand, K. Wouters-Wasiak, P. Baptiste, A. Héduit, Fine bubble aeration with EPDM membranes: conclusions from 15 years of practice, in: IWA Specialized Conference Nutrient Management in Wastewater Treatment Processes and Recycle Streams, Krakow, Poland, 2005, pp. 607–616.
[3] Simon, S., 2000. Etude d'un chenal d'oxydation par des approches globales et locales—Hydrodynamique et transfert de matière. Thèse de doctorat. INSA, Toulouse, 188 p. + annexes.
[4] A. Cockx, Z. Do-Quang, J.M. Audic, A. Liné, M. Roustan, Global and local mass transfer coefficients in waste water treatment process by computational fluid dynamics, Chemical Engineering and Processing 40 (2001) 187–194.
[5] S. Vermande, K. Essemiani, J. Meinhold, C. De Traversay, C. Fonade, Trouble shooting of agitation in an oxidation ditch: applicability of hydraulic modeling, in: 76th Annual Technical Exhibition and Conference WEFTEC'03, October 11–15, Los Angeles, USA, 2003.
[6] S. Vermande, M. Chaumaz, S. Marsal, L. Dumoulin, K. Essemiani, J. Meinhold, Modélisation numérique d'un bassin à grande profondeur. Récent progrès en Génie des Procédés 92, 2005, 8 pp.
[7] Y. Fayolle, S. Gillot, A. Cockx, M. Roustan, A. Héduit, In situ local parameter measurements for CFD modelling to optimize aeration, in: 79th Annual Technical Exhibition and Conference WEFTEC'06, October 21–25, Dallas, USA, 2006, 12 pp.
[8] G. Déronzier, P. Duchène, Vérification de la vitesse horizontale dans les chenaux d'épuration pourvus d'un système d'aération par insufflation d'air, TSM 3 (1997) 35–41.
[9] ASCE, Standard Measurement of Oxygen Transfer in Clean Water, American Society of Civil Engineers, 1992, 41 pp.
[10] NF-EN-12255-15, Wastewater Treatment Plants. Part 15. Measurements of the Oxygen Transfer in Clean Water in Aeration Tanks of Activated Sludge Plants, 2004.
[11] J.P. Giovannettone, J.S. Gulliver, Gas transfer and liquid dispersion inside a deep airlift reactor, AIChE Journal 54 (4) (2008) 850–861.
[12] S. Gillot, S. Capela, A. Héduit, Alpha factor and in-process efficiency in horizontal-flow aeration basins, in: Aeration Conference, Rome, 1998.
[13] S. Gillot, S. Capela, A. Héduit, Effect of horizontal flow on oxygen transfer in clean water with surfactants, Water Research 34 (2) (2000) 678–683.
[14] S. Moustiri, G. Hebrard, S.S. Thakre, M. Roustan, A unified correlation for predicting liquid axial dispersion coefficient in bubble columns, Chemical Engineering Science 56 (3) (2001) 1041–1047.
[15] A. Hasanen, P. Orivuori, J. Aittamaa, Measurements of local bubble size distributions from various flexible membrane diffusers, Chemical Engineering and Processing 45 (4) (2006) 291–302.
[16] G.C. Glover, C. Printemps, K. Essemiani, J. Meinhold, Modelling of wastewater treatment plants—how far shall we go with sophisticated modelling tools? Water Science and Technology 53 (3) (2006) 79–89.
[17] J.P. Giovannettone, E. Tsai, J.S. Gulliver, Gas void ratio and bubble diameter inside a deep airlift reactor, Chemical Engineering Journal 149 (1–3) (2009) 301–310.
[18] G. Déronzier, S. Gillot, P. Duchène, A. Héduit, Influence de la vitesse horizontale du fluide sur le transfert d'oxygène en fines bulles dans les bassins d'aération, Tribune de l'eau (1996) 5–6.
[19] K. Loubière, V. Castaignède, G. Hébrard, M. Roustan, Bubble formation at a flexible orifice with liquid cross-flow, Chemical Engineering and Processing 43 (6) (2004) 717–725.
[20] M. Roustan, A. Liné, Rôle du brassage dans les procédés biologique d'épuration, Tribune de l'eau 5–6 (1996) 109–115.